IOP Conf. Series: Materials Science and Engineering **735** (2020) 012022 doi:10.1088/1757-899X/735/1/012022

Magnetism of Undoped ZrO_2 Nanoparticles Deposited by Plasma-Gas-Condensation Technology

Wenxin Zhou, Kangqi Lin, Laisen Wang*, Qing Luo and Dongliang Peng

College of Materials, Xiamen University, Xiamen 361005, P. R. China
Email: wangls@xmu.edu.cn

Abstract. The magnetic properties of undoped ZrO_2 nanoparticles (NPs) deposited by plasma-gas-condensation technology were studied. The as-prepared ZrO_2 NPs with controllable particle sizes (6-13 nm) presents tetragonal phase which was hardly acquired by traditional methods at room temperature. The as-deposited ZrO_2 NPs were annealed at 300 to 1000 ^oC in air or mixed gas of Ar (95%) + H_2 (5%) for 3 h, respectively. XRD results show that the phase of ZrO_2 NPs gradually transformed from tetragonal to monoclinic with increasing the annealing temperature. The magnetic results of ZrO_2 NPs under all annealing treatments were paramagnetic, which are different with the diamagnetic or ferromagnetic ones, also different from magnetic property changed after annealing in some other works.

1. Introduction

Although unanticipated room-temperature ferromagnetism was found in many nonmagnetic metal oxide nanostructural materials without any doping [1-10], the origin of ferromagnetism still maintained debatable. Thanks to the wide band gap, thermally stability and high dielectric constant [11], ZrO_2 has a promising future in spintronics material and was being studied as the gate-dielectric in field effect transistors [12, 13]. Therefore, studying on the magnetic properties of undoped ZrO_2 is of great academic and practical significance.

Due to the possible undetected ferromagnetic impurities, the controversy in the ferromagnetism of nonmagnetic metal oxide nanostructural materials mainly embodied on whether the ferromagnetic was intrinsic [14-16]. For example, Hadacek *et al.* [14] and Abraham *et al.* [15] consider that ferromagnetism in such materials arise from the ferromagnetism impurity contamination. However, the coercivity detected in such materials is too small to distinguish the ferromagnetic is intrinsic or extrinsic. Meanwhile, creation mechanism of this ferromagnetism in such undoped materials was diversiform without a consensus. For example, Rao *et al.* [3, 6] consider that the exchange interactions of unpaired electron spins resulting from superficial oxygen vacancies generate the ferromagnetism. Coey *et al.* [1, 2] consider that the necessary ferromagnetic coupling is obtained from the polarized impurity band formed by defect-related electrons. Sanvito *et al.* [5] and Gallego *et al.* [17] consider that cation vacancy is the origin of this ferromagnetism by means of *ab initio* calculation. Therefore, for clarifying the origin of ferromagnetism in undoped nonmagnetic metal oxide nanostructural materials, a preparation method which can synthesize high purity nanosacle samples and systematically study on effects of defect on magnetic properties of such materials are necessary.

In this work, the plasma-gas-condensation technology [18] was used to synthesize ZrO_2 nanoparticles with uniform morphology and controllable particle diameters. The as-prepared undoped ZrO_2 NPs are surface clean and contamination free thanks to the vacuum condition and organic-free in

the gas-phase synthesis process. Therefore, the preparation method in our work is very suitable for studying the magnetic properties of such undoped nonmagnetic metal oxide nanostructural materials because the impurity interference can be ignored. In this work, we not only ensure the purity of samples in preparation but also focus on all possible pollution in handling or measurement procedures, especially ensure that there is no contamination on account of using iron based tools in any step of sample processing. As done by many studies, systematic and various annealing treatment were applied to our ZrO_2 NPs for observing changes of magnetic properties.

2. Experimental

2.1. Deposition of ZrO_2 Nanoparticles

During the process of gas-phase synthesis, high density Zr vapor was produced by two Zr targets (99.99%) fixed oppositely with a dc sputtering source. For obtaining nanoparticles with various morphology, the different Ar gas flow rate were imported into sputtering chamber with the fixed sputtering current 0.8 A. The sputtered Zr atoms nucleated and grew by colliding each other and then flew into deposition chamber, finally landed onto the substrates and grew into nanoparticles. The deposition rate of ZrO_2 nanoparticles was measured by the quartz oscillator thickness monitor. The equivalent thickness of ZrO_2 particles assembling films can be estimated by the deposition time and deposition rate. The Zr nanoparticles with controllable sizes were obtained by changing the flow rate of Ar gas. Due to high surface activity, the as-prepared Zr NPs at initial deposition stage completely oxidized to tetragonal ZrO_2 when removed from the deposition device. For studying the magnetic performance of ZrO_2 NPs with different crystal structure and defect concentration, the as-deposited samples were annealed at 300 to 1000 ^{o}C in air and mixed gas of Ar(95%)+H_2(5%) for 3 h, respectively.

2.2. Measurement of ZrO_2 NPs Properties

Transmission electron microscopy (TEM) of JEOL-2100 was employed to studied ZrO_2 NPs with thickness of about 2 nm deposited on TEM copper grids. Surface morphology of NPs with thickness of 400 nm was tested by scanning electron microscope (SEM) LEO-1530FE. The crystalline structures of ZrO_2 NPs on quartz glasses before and after annealing were investigated by a Panalytical X'pert PRO X-ray diffractometer. The MPMS was used to investigate the magnetic hysteresis loops of ZrO_2 NPs with effective thickness of about 400 nm at 5K.

3. Results and Discussion

The TEM images of ZrO_2 NPs prepared with Ar gas flow rate of 200 to 500 sccm deposited on TEM copper grids with effective thickness about 2 nm are shown in **Figure 1(a)**. The corresponding statistical results of size distribution and average particle diameter (*d*) estimated by image-analysis software are shown in **Figure 1(b)**. It can be seen that ZrO_2 NPs prepared at different R_{Ar} had a narrow size distribution and the average diameters were controlled between 6.3 to 12.7 nm. The average particle diameter *d* increases with increasing the flow rate of R_{Ar}. In the synthesis process, Ar gas is used as sputtering and condensation gas at the same time. As the increasing of R_{Ar}, quantity of Zr vapor and Zr-Ar collision probability increases and then the growth of ZrO_2 NPs are promoted. If the ZrO_2 NPs continuously deposited onto the silicon, the nanoparticles assembling films were obtained. It can be seen from the SEM image (Figure. 2) that ZrO_2 nanoparticles-assembled thin films deposited on Si wafer with effective of about 400 nm are accumulated continually by lots of tiny ZrO_2 particles.

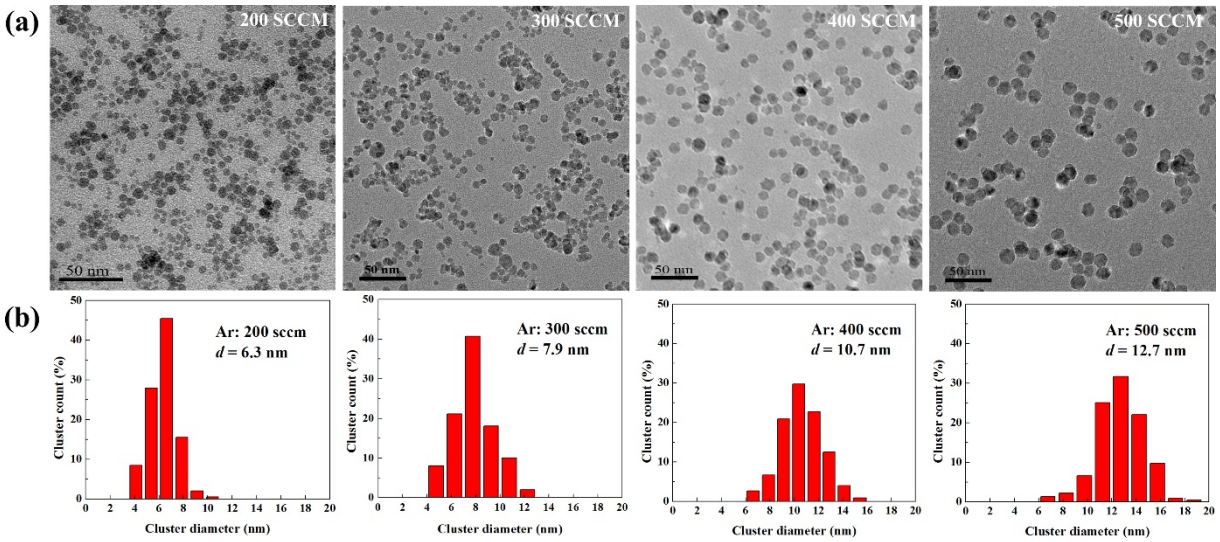

Figure 1. The TEM Images (a) and Corresponding Size Distribution (b) of ZrO_2 Nanoparticles Obtained with Different R_{Ar}

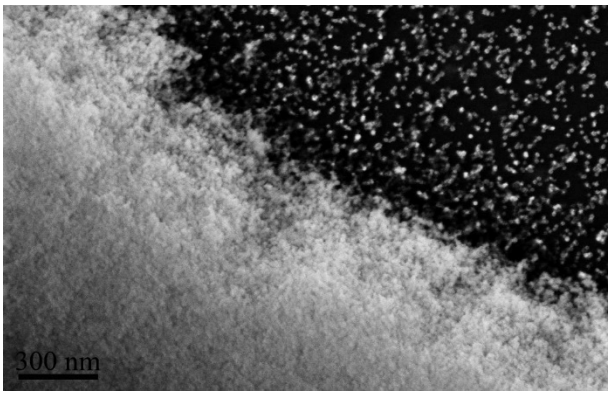

Figure 2. SEM Image of ZrO_2 NPs Assembling Films with Effective Thickness of 400 nm Prepared at R_{Ar} = 200 sccm and I = 0.8 A.

Figure 3(a) presents the XRD pattern of as-prepared ZrO_2 NPs (d = 6.3 nm) deposited on glass with thickness of 400 nm. Compared with the pattern of pure quartz glass (blue line in Figure3 (a)), the ZrO_2 emerges the peak of tetragonal ZrO_2 (101) crystal plane. Because of small size, high defect concentration and poor crystallinity the diffraction peak broadens seriously, but this condition can be improved well by annealing. In normal case, bulk ZrO_2 is stable with monoclinic phase instead of tetragonal phase below 1170 ^oC under normal atmospheric conditions [19]. Owing to dimension effect, the as-prepared ZrO_2 NPs possess high defect concentration and surface energy. For reducing the system energy of NPs, ZrO_2 revealed the high temperature phase (tetragonal) at ambient pressures and temperatures [20-23]. Thus, the undoped tetragonal ZrO_2 which was difficult to obtain at room temperature via traditional synthetic methods can be synthesized by plasma-gas-condensation. **Figure 3(b)** shows the magnetization curve of ZrO_2 NPs on Si substrate. It can be seen that pure Si substrate reveals obvious diamagnetic (red line in Figure 3(b)). After eliminating the diamagnetic signal of Si substrate, the magnetization curve of as-prepared ZrO_2 NPs is almost linear. This indicates that the tetragonal ZrO_2 NPs with average diameter of 6.3 nm is paramagnetic. This result is not in agreement with ferromagnetism [1-10] or diamagnetism [15] found by many similar studies.

In the study of diluted magnetic oxides, the magnetic properties are closely related to the crystal

structure and defects [5, 24]. According some reports, the ferromagnetism nanoscale HfO_2 or ZrO_2 usually present monoclinic phase [2] rather than tetragonal phase in our ZrO_2 NPs. Therefore, for studying the effects of crystal structure, crystallinity and oxygen vacancy on magnetic properties, as-prepared ZrO_2 NPs were annealed in air from 300 to 1000 ^oC for 3 h, respectively. The XRD patterns of ZrO_2 NPs annealed with various temperatures are shown in **Figure 3(c)**. This indicated that the crystallinity of tetragonal ZrO_2 NPs was greatly improved as annealing temperature increased. At the annealing temperature of 800 ^oC, ZrO_2 NPs still maintain tetragonal phase so that the pure tetragonal ZrO_2 at low temperature can be study by plasma-gas-condensation technology. After annealing at 1000 ^oC in air for 3 h, part of ZrO_2 transformed into monoclinic phase from tetragonal phase. The corresponding magnetic properties of ZrO_2 NPs annealed at various temperatures in air were measured by SQUID at 5 K (**Figure 3(d)**). All the magnetic results indicate that ZrO_2 NPs are paramagnetic after all annealing treatments despite it is tetragonal or monoclinic phase, poor or good crystallinity. Furthermore, defect concentration especially oxygen vacancy decreased with the increase of annealing temperature in air (oxidizing atmosphere). Therefore, air-annealing couldn't change the magnetic property of ZrO_2 NPs which is not in agreement with some similar studies [1, 4, 7, 8, 25].

Some researchers also consider that for achieving ferromagnetism in nanoscale oxide, the vacancy concentration of the system should be high [26-28]. For further study on effects of high oxygen vacancy on magnetic properties, ZrO_2 NPs were annealed in reducing atmosphere (mixed gas of Ar(95%) and H_2(5%)) from 300 to 1000 ^oC for 3 h, respectively. A similar XRD results are shown in **Figure 3(e)**. As annealing temperature increased, crystallinity of tetragonal ZrO_2 NPs was greatly improved and transformed into monoclinic phase at the annealing temperature of 1000 ^oC. **Figure 3(f)** shows the corresponding magnetization curves. It can be seen that the magnetic properties still maintain paramagnetic although the paramagnetic moment decreased slightly. Therefore, the increasing oxygen vacancy obtained by annealing in reducing atmosphere couldn't change paramagnetic result to ferromagnetism.

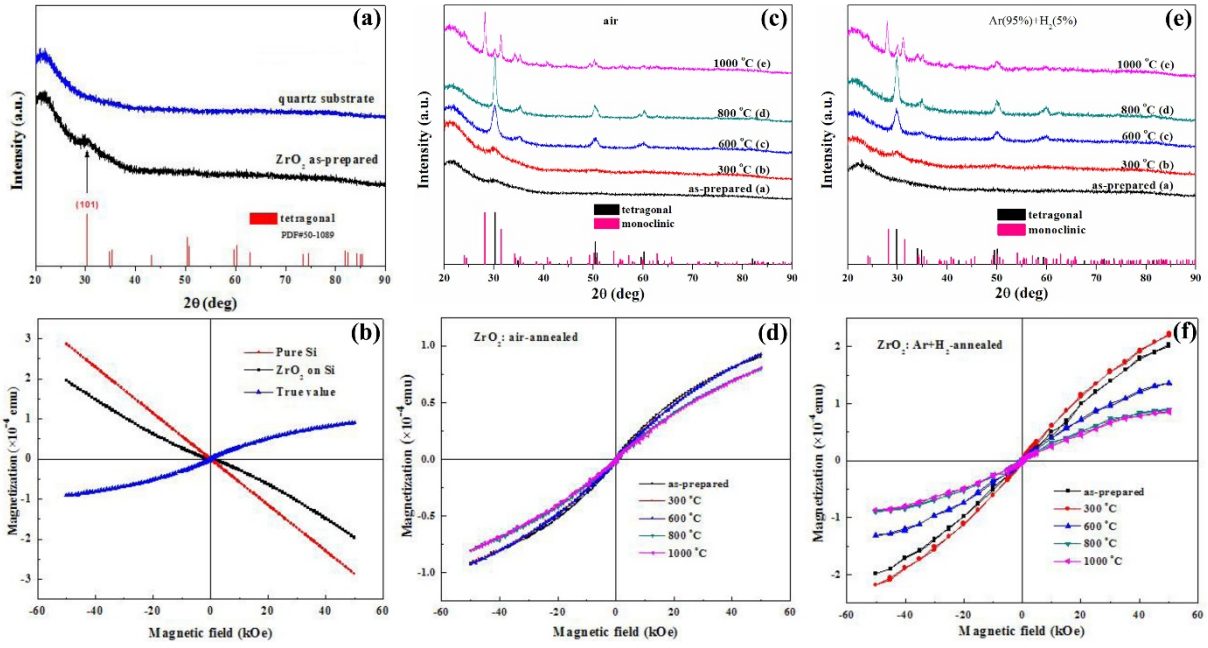

Figure 3. (a) XRD patterns and (b) magnetization curves of as-prepared ZrO_2 NPs deposited on quartz glass and pure Si substrates, respectively. (c) XRD patterns and (d) magnetization curves of ZrO_2 NPs before and after annealing in air atmosphere for 3 h at various temperatures, respectively. (e) XRD patterns and (f) magnetization curves of ZrO_2 NPs before and after annealing in mixed gas of Ar (95%) and H_2 (5%) for 3 h at various temperatures, respectively.

As described above, the ZrO_2 NPs with effective thickness of 400 nm and average diameter of 6.3 nm deposited on Si substrate presents paramagnetic instead of diamagnetism or ferromagnetism reported in recent research. Similar paramagnetic behavior has also been found in HfO_2 by Tirosh *et al*. [25] and copper-doped ZrO_2 by Dutta *et al.* [29], in which this result was regarded as defect or vacancy related. The extended defects might create delocalized and spin-polarized states and then generate magnetic moment [30]. As a result of size-effect, there is a large aggregate superficial area and defect concentration in ZrO_2 nanoparticles. Therefore, we think that the observed paramagnetic behavior in ZrO_2 NPs should be also defect related. However, the paramagnetic result rather than ferromagnetism might be because magnetic properties of undoped nonmagnetic metal oxide nanostructural materials are related with their preparation method, and ferromagnetic results might have stringent demands on morphology, defect types, defect concentration and distribution in such nanostructural materials.

The paramagnetic was maintained even when crystal structure, crystallinity and oxygen vacancy concentration changed after annealing at different temperatures and atmosphere (see Figure 3). This indicates that the paramagnetic of undoped ZrO_2 NPs prepared by plasma-gas-condensation method is stable and rarely affected by the change of crystal structure, crystallinity and oxygen vacancy concentration. This is not the same with magnetism changed from ferromagnetic or paramagnetic to antimagnetic after annealing treatments detected by Coey and Tirosh [1, 25], respectively. Therefore, further work on the clarification of the diamagnetic behavior in such nanoscale material synthesized by gas-phase method is underway.

4. Conclusions

In our work, tetragonal ZrO_2 nanoparticles with uniform morphology and controllable particle diameters (6-13 nm) through modifying the flow rate of Ar gas were prepared by plasma-gas-condensation technology. After annealing at different temperatures in oxidizing or reducing atmosphere for 3h, respectively, tetragonal ZrO_2 partly converted into monoclinic phase at the annealing temperature of 1000 ^{o}C and their magnetic properties remained paramagnetic despite the change of crystal structure, crystallinity and oxygen vacancy concentration. The paramagnetic result in our work is different with the ferromagnetic or diamagnetic one, also different from magnetic property changed after annealing treatments in some reports. However, whether this experimental phenomenon also applies to every such nanoscaled materials with different morphologies and dimensions, this interesting result provides a new experimental phenomenon and basis for the study on magnetic properties of undoped nonmagnetic metal oxide materials.

5. Acknowledgements

This work was supported by the National Natural Science Foundation of China (Grant No. 51771157, 51571167 and 51901197), the Fundamental Research Funds for the Central Universities of China (Xiamen University: Nos. 20720190007).

6. References

[1] Coey J.M.D., Venkatesan M., Stamenov P., Fitzgerald C.B. and Dorneles L.S. 2005 *Phys. Rev. B* **72** 024450.
[2] Venkatesan M., Fitzgerald C.B. and Coey J.M.D. 2004 *Nature* **430** 630.
[3] Sundaresan A., Bhargavi R., Rangarajan N., Siddesh U. and Rao C.N.R. 2006 *Phys. Rev. B* **74** 161306.
[4] Ma N.G., Zhang Y.J., Cao E.S., Sun L., Hao W.T. and Yang Z. *Chem. Phys. Lett.* 2019 **727** 6-104.
[5] Pemmaraju C.D. and Sanvito S. 2005 *Phys. Rev. Lett.* **94** 217205.
[6] Sundaresan A. and Rao C.N.R. 2009 *Nano Today* **4** 96-106.
[7] Yi J.B., Pan H., Lin J.Y., Ding J., Feng Y.P., Thongmee S., Liu T., Gong H. and Wang L. 2008 *Adv. Mater.* **20** 1170-1174.
[8] Nandy A., Pal U. and Pradhan S.K. 2019 *J. Alloy. Compd.* **793** 220-231.
[9] Esmaeily A.S., Venkatesan M., Sen S. and Coey J.M.D. 2018 *Phys, Rev. Mater.* **2** 054405.

[10] Gao Q., Chen H.L., Li K.F. and Liu Q.Z. 2018 *ACS Appl. Mater. Inter.* **10** 27503-27509.
[11] Seema K. and Kumar R. 2015 *J. Supercond. Nov. Magn.* **28** 2735-2742.
[12] Ostanin, S. *et al.*, 2007 *Phys. Rev. Lett.* **98** 016101.
[13] Konda R.B., White C., Smak J., Mundle R., Bahoura M. and Pradhan A.K. 2013 *Chem. Phys. Lett.* **583** 74.
[14] Hadacek N., Nosov A., Ranno L., Strobel P and Gal´era R-M 2007 *J. Phys. Condens. Matter* **19** 486206 14.
[15] Abraham D.W., Frank M.M. and Guha S. 2005 *Appl. Phys. Lett.* **87** 252502.
[16] Jo Y., Hwang I.R., Park B.H., Lee K.J., Lee S.I. and Jung M.H. 2009 *Appl. Phys. Lett.* **95** 263504
[17] Gallego S., Beltr´an J.I., Cerd´a J and Mu˜noz M.C. 2005 *J. Phys. Condens. Matter* **17** 451–457.
[18] Wang L.S., Wen R.T., Chen Y., Yue G.H. and Peng D.L. 2011 *Appl. Phys. A* **103** 1015.
[19] Yoshimura M. 1988 Am. Ceram. Soc. Bull. **67** 1950.
[20] Garvie R.C. and Goss M.F. 1986 J. Mater. Sci. **21** 1253.
[21] Bokhimi X., Morales A., Novaro O., Portilla M., López T., Tzompantzi F. and Gómez R. 1998 *J. Solid. State. Chem.* **135** 28-35.
[22] Duwez P., Odell F. and Brown F.H. 1952 *J. Am. Ceram. Soc.* **35** 107.
[23] Duwez P., Brown F.H. and Odell F. 1951 *J. Electrochem. Soc.* **98** 356.
[24] Ye L.H. and Freeman A. J. 2006 *Phys. Rev. B* **73** 081304.
[25] Tirosh E. and Markovich G. 2007 *Adv. Mater.* **19** 2608-2612.
[26] Maoz B.M., Tirosh E., Sadan M.B. and Markovich G. 2011 *Phys. Rev. B* **83** 161201.
[27] Zunger A., Lany S. and Raebiger H. 2010 *Physics* **3** 53.
[28] De Souza A.O., Ivashita Flávio F., Biondo V., Paesano A. and Mosca D.H. 2016 *J. Alloy. Compd.* **680** 701-710.
[29] Dutta P., Seehra M. S., Zhang Y. and Wender I. 2008 *J. Appl. Phys.* **103** 07D10428.
[30] Schoenhalz A.L., Arantes J.T., Fazzio A. and Dalpian G.M. 2009 *Appl. Phys. Lett.* **94** 162503 30.